

AD-A284 561



RL-TR-93-221
In-House Report
October 1993



NUMERICALLY EFFICIENT USE OF FREQUENCY DOMAIN MoM CODES FOR WIDEBAND RADIATION AND SCATTERING PROBLEMS - AN APPLICATION: SCATTERING FROM A MICROSTRIP PATCH

Hans Steyskal and Richard C. Hall

DTIC
ELECTE
SEP 20 1994
S G D

APPROVED FOR PUBLIC RELEASE; DISTRIBUTION UNLIMITED.

94-30217



DTIC QUALITY INSPECTED 3

348
Rome Laboratory
Air Force Materiel Command
Griffiss Air Force Base, New York

94 0 16 86

This report has been reviewed by the Rome Laboratory Public Affairs Office (PA) and is releasable to the National Technical Information Service (NTIS). At NTIS it will be releasable to the general public, including foreign nations.

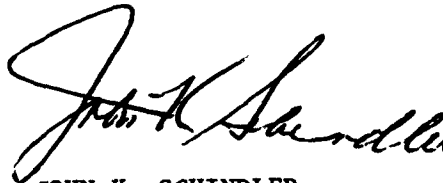
RL-TR-93-221 has been reviewed and is approved for publication.

APPROVED:



DANIEL J. JACAVANCO
Chief, Antennas & Components Division
Electromagnetics & Reliability Directorate

FOR THE COMMANDER:



JOHN K. SCHINDLER
Director of Electromagnetics & Reliability

If your address has changed or if you wish to be removed from the Rome Laboratory mailing list, or if the addressee is no longer employed by your organization, please notify RL (ERAA) Hanscom AFB MA 01731. This will assist us in maintaining a current mailing list.

Do not return copies of this report unless contractual obligations or notices on a specific document require that it be returned.

REPORT DOCUMENTATION PAGE			Form Approved OMB No. 0704-0188	
Public reporting burden for this collection of information is estimated to average 1 hour per response, including the time for reviewing instructions, searching existing data sources, gathering and maintaining the data needed, and completing and reviewing the collection of information. Send comments regarding this burden estimate or any other aspect of this collection of information, including suggestions for reducing this burden, to Washington Headquarters Services, Directorate for Information Operations and Reports, 1215 Jefferson Davis Highway, Suite 1204, Arlington, VA 22202-4302, and to the Office of Management and Budget, Paperwork Reduction Project (0704-0188), Washington, DC 20503.				
1. AGENCY USE ONLY (Leave blank)		2. REPORT DATE October 1993		3. REPORT TYPE AND DATES COVERED In-House February 1992 - September 1993
4. TITLE AND SUBTITLE Numerically Efficient Use of Frequency Domain MoM Codes for Wideband Radiation and Scattering Problems - An Application: Scattering From a Microstrip Patch			5. FUNDING NUMBERS PR 2304 TU: I3 WU: 02 PE: 61102F	
6. AUTHOR(S) H. Steyskal R. C. Hall*				
7. PERFORMING ORGANIZATION NAME(S) AND ADDRESS(ES) Rome Laboratory (ERAA) 31 Grenier Street Hanscom AFB, MA 01731-3010			8. PERFORMING ORGANIZATION REPORT NUMBER RL-TR-93-221	
9. SPONSORING/MONITORING AGENCY NAME(S) AND ADDRESS(ES)			10. SPONSORING/MONITORING AGENCY REPORT NUMBER	
11. SUPPLEMENTARY NOTES * Huber + Suhner AG, CH-9100 Herisau, Switzerland Rome Lab POC: Hans Steyskal/ERAA, (617) 377-2052				
12a. DISTRIBUTION/AVAILABILITY STATEMENT Approved for Public Release; Distribution Unlimited			12b. DISTRIBUTION CODE	
13. ABSTRACT (Maximum 200 words) A concise and numerically efficient method for the wide band or transient characterization of three-dimensional antennas or scatterers is presented. Assuming a situation where a frequency domain Method of Moment code already exists for the particular structure of interest, we extend the code to accept complex frequencies and use it to compute the natural resonances and modes. The desired wide-band spectrum is then expanded in terms of these modes, and the unknown expansion coefficients (the crux in any application of the Singularity Expansion Method) are determined by a least mean square match to a known reference case, also obtained with the existing code. The computational issues involved in using this approach are discussed. As an example, an analytic approximation for the radar cross section of a microstrip patch valid over the 1-18 GHz range is derived, which uses only 15 natural modes.				
14. SUBJECT TERMS Wideband scattering, Microstrip patch radar cross section, Natural mode expansion, SEM			15. NUMBER OF PAGES 34	
			16. PRICE CODE	
17. SECURITY CLASSIFICATION OF REPORT UNCLASSIFIED	18. SECURITY CLASSIFICATION OF THIS PAGE UNCLASSIFIED	19. SECURITY CLASSIFICATION OF ABSTRACT UNCLASSIFIED	20. LIMITATION OF ABSTRACT UL	

Contents

1. INTRODUCTION	1
2. FORMULATION OF THE APPROACH	3
3. EXAMPLE: THE RADAR CROSS SECTION OF A MICROSTRIP	5
4. RESULTS AND DISCUSSION	8
5. CONCLUSION	19
REFERENCES	23
APPENDIX	
The k_0 -dependence of the Radar Cross Section of a Microstrip Patch at Low Frequencies	25

Accession For	
NTIS	CRA&I <input checked="checked" type="checkbox"/>
DTIC	TAB <input type="checkbox"/>
Unannounced <input type="checkbox"/>	
Justification	
By	
Distribution /	
Availability Codes	
Dist	Avail and/or Special
A-1	

Illustrations

1. Geometry of Air Loaded Microstrip Patch and Incident Plane Wave.	4
2. First Family Pole Locations in the Complex Frequency Plane for the Patch of Figure 1.	9
3. Second Family Pole Locations in the Complex Frequency Plane for the Patch of Figure 1.	10
4. Convergence of the First Family of Poles in the Complex Frequency Plane for Different Numbers of Moment Method Basis Functions.	11
5. a) In-phase and Quadrature Phase Current Components for the Seventh Natural Mode of the Patch Shown in Figure 1, Corresponding to the TM_{120} Cavity Mode.	12
b) In-phase and Quadrature Phase Current Components for the 15:th Natural Mode, Corresponding to the TM_{500} Cavity Mode.	13
6. Comparison of the RCS Calculated Using the SEM Current Model and the Exact MoM Model for the Patch of Figure 1. The SEM current model is matched to the MoM currents at one frequency and two frequencies.	15
7. Comparison of the RCS Calculated Using the SEM Current Model and the Exact MoM Model for the Patch of Figure 1. The SEM current model is matched to the MoM currents at four frequencies.	16
8. In-phase Components of Patch Current as Obtained With Exact MoM Computation (Top) and With a Seven Mode Expansion (Bottom), at 10 GHz.	17
9. Comparison of the RCS Calculated Using the SEM Current Model and the Exact MoM Model for the Patch of Figure 1. The SEM current model is matched to the MoM currents at eight frequencies.	18
10. Same Case as Figure 7, Except That the SEM Current Model has Been Modified to Include a DC Correction Term.	20
11. Bistatic RCS at 16 GHz Calculated Using the SEM Current Model and the Exact MoM Model for the Patch in Figure 1.	21
A1. Scattering From a Microstrip Patch Related to a Patch Pair in Free Space.	27

Table

1. Cavity Resonances and Corresponding Complex Poles.

14

Acknowledgements

A significant part of this study was performed while one of us (Steyskal), was on a research visit at the Swiss Federal Institute of Technology, Lausanne, Switzerland with support from the US Air Force Office of Scientific Research. R. Hall was supported by Huber + Suhner AG, Switzerland.

Numerically Efficient Use of Frequency Domain MoM Codes For Wideband Radiation and Scattering Problems – An Application: Scattering From a Microstrip Patch

1. INTRODUCTION

With the present interest in electromagnetic pulses the question arises whether existing frequency-domain computer codes can be used to provide the temporal response of antennas and scatterers.

These codes, which usually are based on the Method of Moments (MoM), are highly accurate and also represent a large investment in both financial resources and development time. Of course, since time and frequency domain solutions are related by the Fourier transform, these codes in principle could be used to numerically evaluate the spectrum of the impulse response and, after multiplication with the signal spectrum, an inverse Fourier transform would lead to the desired time domain response. However, the impedance or scattering behavior of many objects is not a smooth function of frequency, especially at frequencies near resonances of the structure, and to capture these rapid variations requires a very dense numerical sampling of the spectrum. This represents a large, and sometimes prohibitively large, computational effort.

Thus, there is a need for a more efficient approach than a straightforward numerical Fourier transform.

The approach proposed here is based on the observation that the late time impulse response of many 3-dimensional structures is often well represented by a set of damped sinusoids [1] that appear as singularities (poles) in the complex frequency plane. This suggests modeling the response by a small set of such complex natural resonances and associated natural modes, rather than by a purely numerical spectrum evaluation. The approach can be viewed as "smart" interpolation since the physically motivated interpolation functions contribute additional information. The method has also been called model-based parameter estimation [2], a term borrowed from signal estimation theory.

The overall approach involves the following three general steps. First, an appropriate number of complex natural resonances for the frequency range of interest and the corresponding natural modes are determined. This is done with the aid of a frequency domain moment method (MoM) code assumed available for the structure under consideration. Second, the induced currents on the structure are expanded in terms of the natural resonances and modes with unknown amplitudes. This is the so-called singularity expansion method (SEM) current estimate. The determination of the mode amplitudes is typically the most difficult step of the overall process [1], [3]. (This is where people usually give up', to quote Dr D Giri, an old master of the art of the SEM). Presently, a new approach is introduced to determine the amplitudes that uses least-squares matching of the current estimate to known or 'trusted reference' currents at several frequencies. The reference currents are produced with the existing MoM code. Finally, the electromagnetic characteristics of interest such as the input impedance or radar cross section (RCS) are calculated from the SEM current estimate. This can be done rapidly over a wide frequency range, due to the simple form of the current estimate.

One of the advantages of our method includes the possibility of using existing frequency domain MoM codes with only slight modifications to calculate the wide band frequency response with reduced computation time. A compact analytic approximation for the spectrum is obtained, from which a direct time domain (pulse) solution of a radiation or scattering problem is easily derived. Since it is assumed that the moment method model of the object has already been developed and tested, little additional coding work is required.

As an example of the application of the hybrid SEM/MoM technique presented here, the radar cross section of a microstrip patch is calculated over the 1-18 GHz band. The numerical evaluation of the radar cross section of microstrip patches in the frequency domain has been studied by several authors [4]-[5]. The agreement between measured and calculated results that these authors have attained has been very good. Nevertheless, the computational effort required in some cases has been quite large. Therefore, several methods have been developed to help reduce the computational burden. These methods have often involved sparse frequency sampling or "smart" interpolation schemes based on additional physical insight or mathematical characteristics. Interpolation of the moment method matrix [4] is one of the earlier methods that was applied with success. In this case, the time required to fill the moment method matrix dominated the calculation so the matrix was filled at only widely spaced frequencies. The moment method matrix was then interpolated at intermediate frequencies and the resulting matrix equation solved for the current at these intermediate frequencies. This interpolation approach is not successful in all cases, however. The addition of a probe attachment basis function causes the method to fail [5]. In addition, matrix interpolation schemes do not help MoM techniques that have relatively short matrix fill times and longer matrix solution times [6]-[7]. In these situations, a result of the matrix equation such as the induced current density rather than the matrix equation itself must be interpolated. However, due to the highly resonant nature of these quantities, this interpolation is exceedingly difficult.

The sections that follow outline the basic formulation, discuss the computational implementation and present computed radar cross section results for a rectangular air loaded microstrip patch over a 18:1 frequency range.

2. FORMULATION OF THE APPROACH

The details of the general approach are outlined in this section.

The currents on a three-dimensional structure such as the microstrip patch shown in Figure 1 can be expanded in terms of its natural resonances ω_m and natural modes $\mathbf{J}_m(\mathbf{r}')$. The natural resonances and corresponding modes are solutions to the homogeneous problem and thus are independent of any incident fields or forcing function. The natural resonances occur as pairs in quadrants I and II of the complex frequency plane and are symmetrically placed about the imaginary axis, (when a frequency plane is chosen such that the real frequency axis corresponds to continuous undamped waves). The poles lie in the upper half-plane so the impulse response decays with time.

The Singularity Expansion Method (SEM) current approximation of the true spectrum $\mathbf{J}(\mathbf{r}', \omega)$ of the impulse response in terms of the natural resonances and modes takes the form

$$\mathbf{J}(\mathbf{r}', \omega) \approx \mathbf{J}_{SEM}(\mathbf{r}', \omega) \equiv$$

$$\sum_{m=1}^M \left[\left(\eta_m \mathbf{J}_m(\mathbf{r}') \frac{1}{\omega - \omega_m} \right) - \left(\eta_m \mathbf{J}_m(\mathbf{r}') \frac{1}{\omega + \omega_m} \right)^* \right] \quad (1)$$

where η_m are the mode amplitudes or coupling coefficients. The amplitudes η_m are determined by the excitation. For the scattering problem, for example, the amplitudes determine how strongly a plane wave incident from a given direction excites the m-th natural mode. The natural resonances, the corresponding natural modes, and the mode amplitudes for a particular excitation are, in general, unknown and must be determined to complete the current approximation $\mathbf{J}_{SEM}(\mathbf{r}', \omega)$.

In theory, the series in Eq. (1) contains an infinite number of natural modes, $M \rightarrow \infty$ and there is also a possible contribution from an entire function. However, in practice a small number of modes often suffices.

Note the convenient separation of the frequency and incident angle dependencies in Eq. (1). This facilitates computing the time domain response of the structure since once the currents are written in this form the multiplication with the spectrum of the desired signal and the inverse Fourier transform to obtain the time response become trivially simple.

The natural frequencies and modes are obtained from the MoM matrix equation that normally takes the form

$$\mathbf{M}(\mathbf{r}', \mathbf{r}, \omega) \mathbf{J}(\mathbf{r}', \omega) = \mathbf{V}(\mathbf{r}, \omega) \quad (2)$$

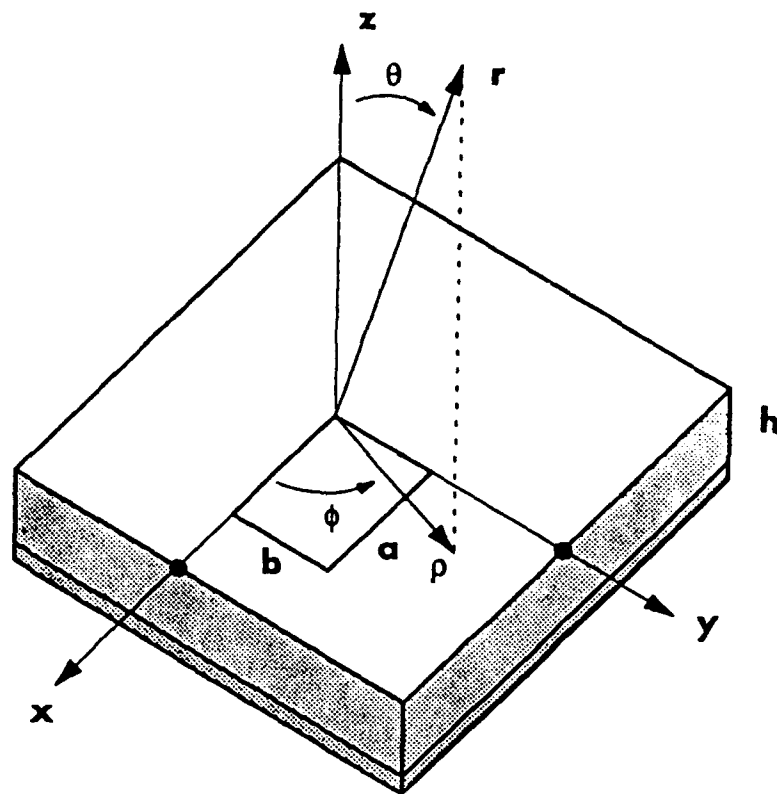


Figure 1. Geometry of Air Loaded Microstrip Patch and Incident Plane Wave.

Patch dimensions: $a = 36.6$ mm, $b = 26.0$ mm

Patch height above ground plane: $h = 1.58$ mm

Plane wave incident angle: $\theta = 60^\circ$, $\phi = 45^\circ$.

where $\mathbf{J}(\mathbf{r}', \omega)$ is the current density vector, $\mathbf{M}(\mathbf{r}, \mathbf{r}', \omega)$ is the moment method impedance matrix and the vector $\mathbf{V}(\mathbf{r}, \omega)$ is related to the particular forcing function that may be, for example, an incident plane wave or voltage gap generator.

The natural resonances ω_m are defined by the matrix $\mathbf{M}(\mathbf{r}, \mathbf{r}', \omega)$ in that they satisfy

$$\det [\mathbf{M}(\mathbf{r}', \mathbf{r}, \omega_m)] = 0 \quad (3)$$

which is a necessary condition for a source-free solution. The corresponding natural modes $\mathbf{J}_m(\mathbf{r}')$ are obtained as the solutions of the matrix equation

$$\mathbf{M}(\mathbf{r}', \mathbf{r}, \omega_m) \mathbf{J}_m(\mathbf{r}') = 0 \quad (4)$$

The evaluation of the unknown amplitudes, the η_m of Eq. (1), is usually the major difficulty, since they essentially involve evaluating the residue of $\mathbf{M}^{-1} \mathbf{V}$ at $\omega = \omega_m$. However, in the present case the available moment method code allows a much simpler, alternate approach. Using this code to generate a CW reference current $\mathbf{J}_{CW}(\omega_n)$ on the patch at a particular real frequency ω_n , the amplitudes can be determined by the condition that the current estimate $\mathbf{J}_{SEM}(\omega_n)$ of Eq. (1) provides a least mean square match to $\mathbf{J}_{CW}(\omega_n)$, that is, the error

$$\epsilon_n(\eta_1, \dots, \eta_M) = \|\mathbf{J}_{SEM}(\omega_n) - \mathbf{J}_{CW}(\omega_n)\|^2 \quad (5)$$

is minimized. In principle all the amplitudes $\{\eta_m\}$ can be determined by matching at one single frequency. However, a more uniform matching over the band of interest obtained by minimizing a combined error from several frequencies

$$\epsilon = \sum_n \epsilon_n(\eta_1, \dots, \eta_M), \quad (6)$$

usually leads to a better result.

Once the currents on the structure are known, the input impedance or radar cross section may easily be calculated.

3. EXAMPLE: THE RADAR CROSS SECTION OF A MICROSTRIP PATCH

In this section the computational issues involved in applying the singularity expansion method to the study of scattering from a microstrip patch will be discussed, since they have a strong influence on the overall success or failure of the method. In addition, important features of the method and its implementation will be further outlined.

The natural resonances were first determined by modifying an existing moment method computer code [6]-[7] to accept complex frequencies. This moment method code is a so-called "full-wave" code that can accurately describe higher-order hybrid current distributions on the patch. The method is based on a mixed potential integral equation and expands the patch currents in a series of "roof-top" shaped basis functions. Typically 130 basis functions are required to accurately model the patch currents at the fourth or fifth resonant frequency. While the matrix fill time is relatively short, the MoM matrix is fairly large and the solution time of the matrix equation grows roughly as N^3 as more basis functions are added to model finer patch details or to study the antenna at higher frequencies.

The natural resonances were determined from Eq. (3), which implies that an eigenvalue of the impedance matrix goes to zero or, equivalently, the condition number goes to infinity. Here the complex frequency plane was searched for maxima of the condition number of the moment method impedance matrix. The Muller method [8] was used for this search while LINPACK [9] routines were used to estimate the condition number. The real resonant frequencies determined by the cavity model were used as starting locations for the Muller method search since the efficiency of this method depends heavily on the quality of the initial starting locations. The cavity model resonances (TM_{pq0}) for a rectangular microstrip antenna are given approximately in GHz by

$$f \cong 0.96 \frac{150}{\sqrt{\epsilon_r}} \left[\left(\frac{p}{a} \right)^2 + \left(\frac{q}{b} \right)^2 \right]^{1/2} \quad (7)$$

where a and b are the dimensions of the patch in millimeters, ϵ_r is the relative permittivity of the substrate, and the factor 0.96 accounts for the difference between a closed cavity and the actual microstrip, which has a fringing field.

The patch shown in Figure 1 was subdivided into a large number of cells (13 by 11 cells leading to a total of 262 rooftop basis functions: 132 x-directed, 130 y-directed) in the moment method code to yield accurate results at the higher frequencies. The search for each complex resonant frequency required approximately 12 evaluations of the moment method matrix condition number. Therefore, finding the first seven natural resonances to cover the 1-12 GHz band required approximately 84 evaluations of the MoM matrix condition number.

The natural modes corresponding to each of the natural resonances were found by use of a matrix deflation technique. At a complex resonance the natural mode is a non-trivial solution to the homogeneous matrix equation (4). To determine this mode one arbitrary mode component is set to a non-zero value, which leads to a reduced set of $N-1$ inhomogeneous equations that can be solved. This determines the natural mode apart from its magnitude, which can be set by normalization. The numerical condition number of the reduced matrix was typically 50 times better than the original "numerically singular" matrix. The computation of each of the natural modes, therefore, requires roughly one evaluation of the MoM matrix equation. (This method can fail if the reduced matrix equation is also numerically singular.)

A second method for determining the natural modes is to compute the eigenvector associated with the minimum eigenvalue of the matrix at a natural resonance. This method produces equally good results but is significantly less efficient computationally.

The same moment method code was then used to calculate the reference current distributions at several real frequencies. The error between the reference moment method currents and the current approximation (Eq. (1)) was minimized to determine the mode amplitudes.

Finally, for the microstrip patch scattering problem considered here, the radar cross section in the polar direction (θ, ϕ) was computed using the natural mode current expansion by

$$\sigma_{TE} = \frac{1}{\pi} |Z_0 k_0^2 A h \cos \theta (F_x \sin \phi - F_y \cos \phi) / E_{inc}|^2 \quad (8a)$$

$$\sigma_{TM} = \frac{1}{\pi} |Z_0 k_0^2 A h \cos^2 \theta (F_x \cos \phi + F_y \sin \phi) / E_{inc}|^2 \quad (8b)$$

where Z_0 is the free space wave impedance, k_0 is the wavenumber, A is the area of a charge cell on the patch (that is, one-half the area covered by a roof-top basis function), h is the height above the ground plane, and F_x and F_y are array factors for the rooftop basis functions on the patch given by

$$F_x = \sum_m J_{xm} e^{jk_0 r'_m \cos \psi} \quad (9a)$$

$$F_y = \sum_n J_{yn} e^{jk_0 r'_n \cos \psi} \quad (9b)$$

The currents J_{xm} and J_{yn} are the x and y directed components of the current approximation (1), and ψ is the angle between the vectors to the field point \mathbf{r} and to the source point \mathbf{r}' . In this derivation it is assumed that $h \ll \lambda$ so that the array factor for the patch, and its negative image in the groundplane, is

$$e^{-jk_0 h \cos \theta} - e^{jk_0 h \cos \theta} \simeq -j2k_0 h \cos \theta$$

The far field for a patch with known current is then calculated following, for instance, van Bladel [10].

The computational effort to evaluate the mode amplitudes was negligible while the computation of the radar cross section of the patch using the current estimates over the entire band was, for the case chosen here, roughly equivalent to one evaluation of the MoM matrix equation. Thus, with the present state of affairs, the computational effort required to implement the SEM and MoM solutions was roughly equivalent at approximately 90 frequencies. SEM is more efficient for a larger number of frequency points while MoM is better for a smaller number of frequencies.

Both the moment method and the singularity expansion method can compute radar cross section efficiently for multiple incident angles. The moment method approach must invert the MoM matrix once, compute the multiple right-hand-sides and multiply. The present technique requires the MoM solution for the reference current at several frequencies for each incident angle to determine the mode amplitudes.

4. RESULTS AND DISCUSSION

The radar cross section of the air-loaded patch of Figure 1, computed by using the natural mode current expansion, is presented in this section and compared to the direct calculation by the moment method. While in principle the present method and the MoM code can be applied to dielectric loaded patch antennas where the substrate of the antenna is not air, questions about surface wave pole migration in the complex plane when studying the antenna at complex frequencies were beyond the scope of the current work. The precise location of the surface wave poles must be known during the calculation of the Sommerfeld integrals that are the Green's functions of the integral equation.

Figure 2 shows the locations of the first 11 members of a family of complex natural resonances that lie near the real frequency axis. The real resonant frequencies predicted by the cavity model that were used as starting locations for the Muller method search and the corresponding mode numbers are also shown. Note the surprisingly close correspondence between the real and complex resonances. (The correspondence was established by comparing the mode current distributions). A list of 15 poles that were found in this family is given in Table 1.

A second family of natural resonances, shown in Figure 3, lies in the complex plane far above the first. These modes play a secondary role in the late time impulse response of the patch and were more difficult to find since there exists no clear starting point for the search. The second family modes were not included in the results that follow.

The convergence of the first family of poles with the number of moment method basis functions is shown in Figure 4. The subdivision of the patch into a larger number of cells improves the convergence of the natural modes at the higher frequencies but does not significantly improve the final radar cross section results. The number of cells chosen here, 13×11 , corresponds to about 9 cells per wavelength at 12 GHz and 6 per wavelength at 18 GHz.

Figure 5a shows a quiver diagram of the in-phase and quadrature-phase components of the seventh natural mode. The complex frequency of this mode is approximately $11.20 + j0.33$ GHz and corresponds to the TM_{120} cavity mode resonant at $f = 11.52$ GHz. We note that the in-phase component is roughly 8 times stronger than the quadrature component. Figure 5b similarly shows the 15:th natural mode, which clearly is seen to corresponds to the TM_{500} cavity mode. This time the in-phase component dominates by a factor of 11.

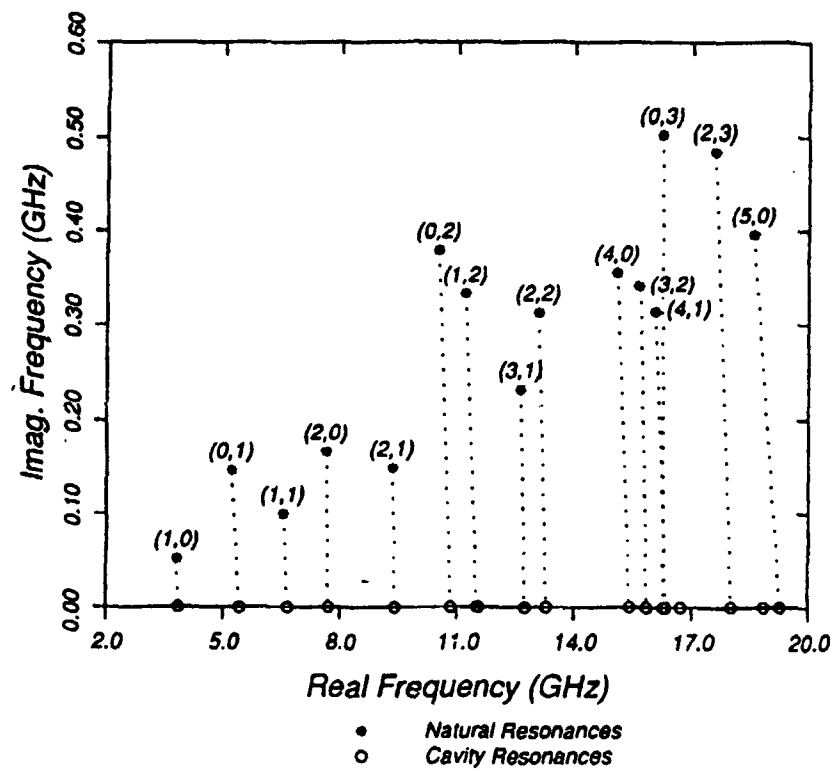


Figure 2. First Family Pole Locations in the Complex Frequency Plane for the Patch of Figure 1. The corresponding resonant frequencies predicted by the cavity model are shown along the real axis.

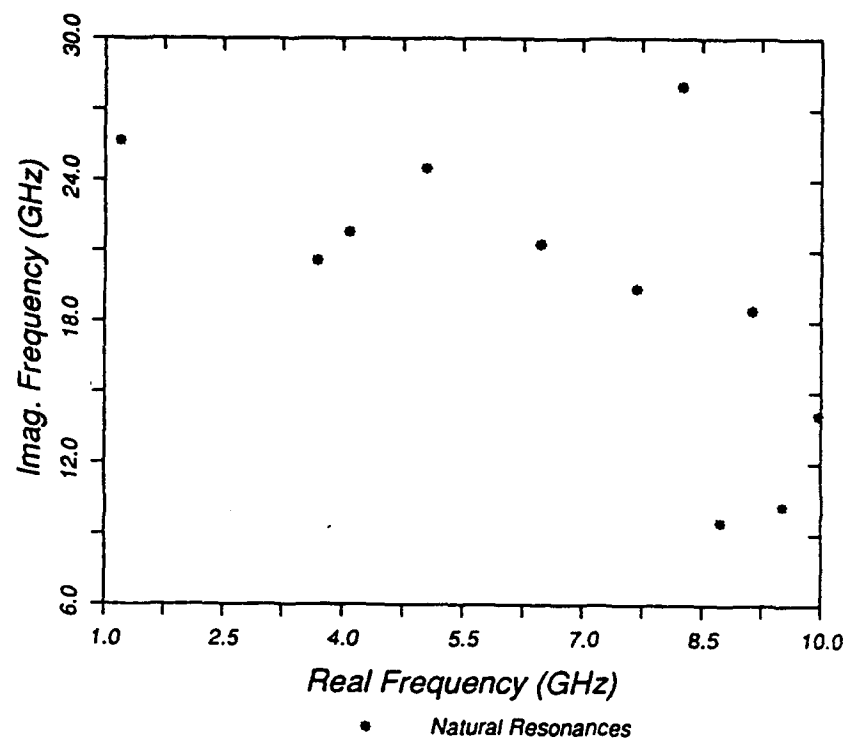


Figure 3. Second Family Pole Locations in the Complex Frequency Plane for the Patch of Figure 1.

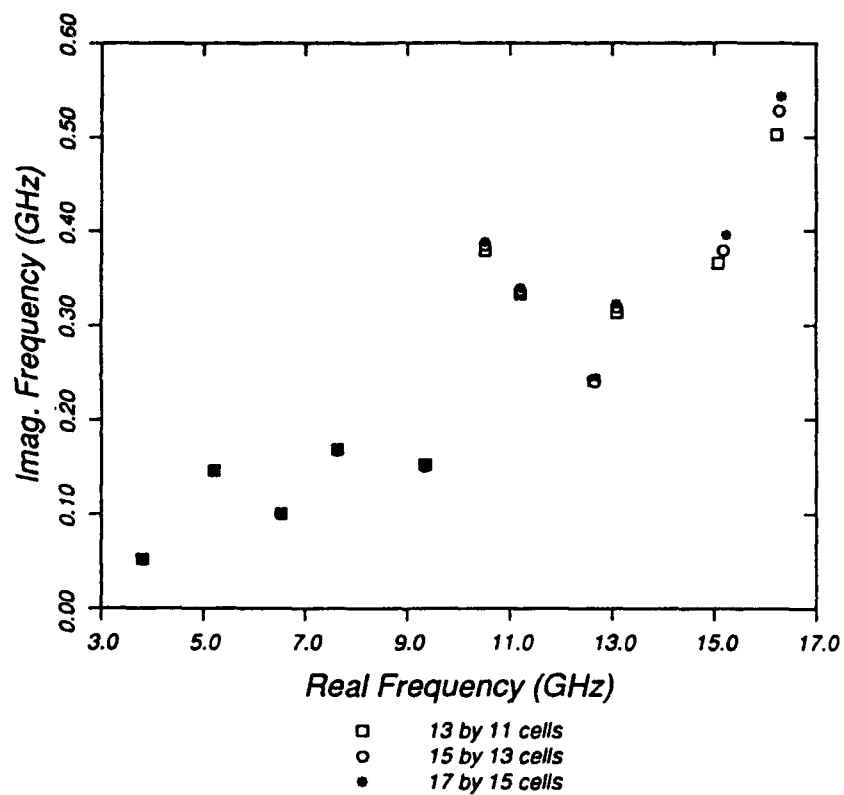
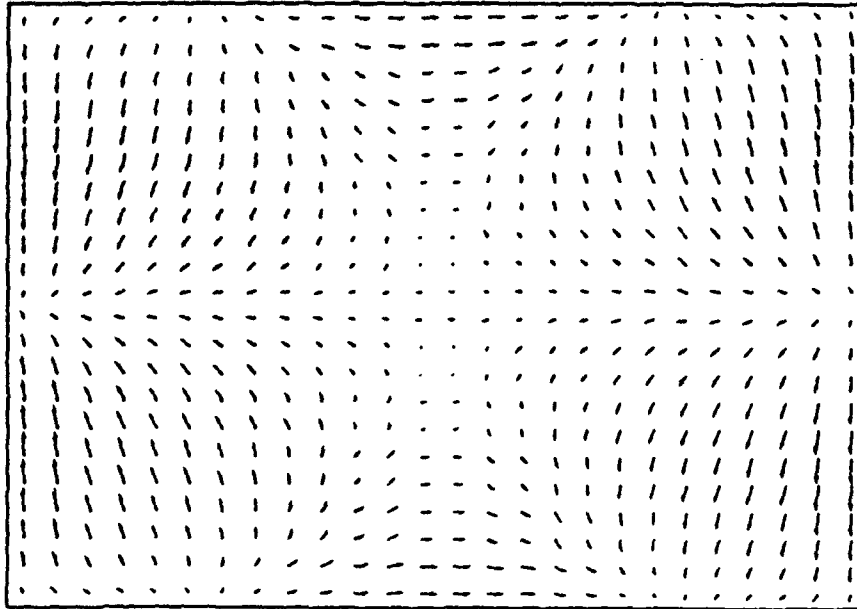


Figure 4. Convergence of the First Family of Poles in the Complex Frequency Plane for Different Numbers of Moment Method Basis Functions.

In-Phase

Max. Value = 1.660×10^0 Amps



Quadrature-Phase

Max. Value = 0.198×10^0 Amps

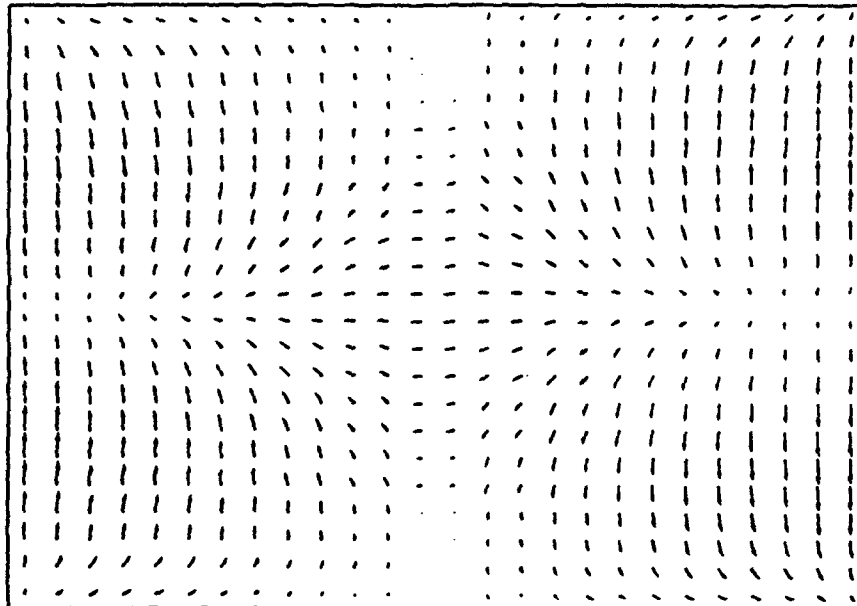
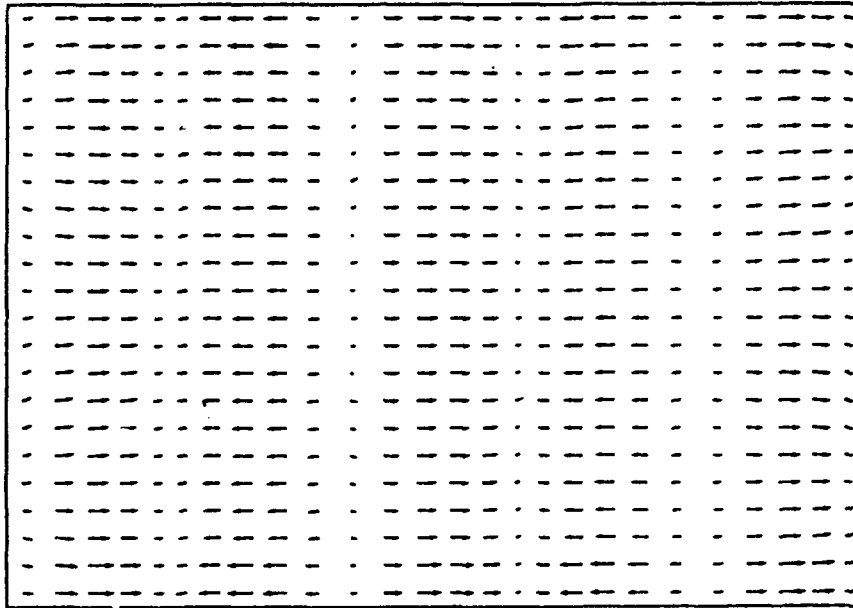


Figure 5a. In-phase and Quadrature Phase Current Components for the Seventh Natural Mode of the Patch Shown in Figure 1. Corresponding to the TM_{120} Cavity Mode.

Max. Value = 0.882×10^0 Amps



Max. Value = 0.799×10^{-1} Amps

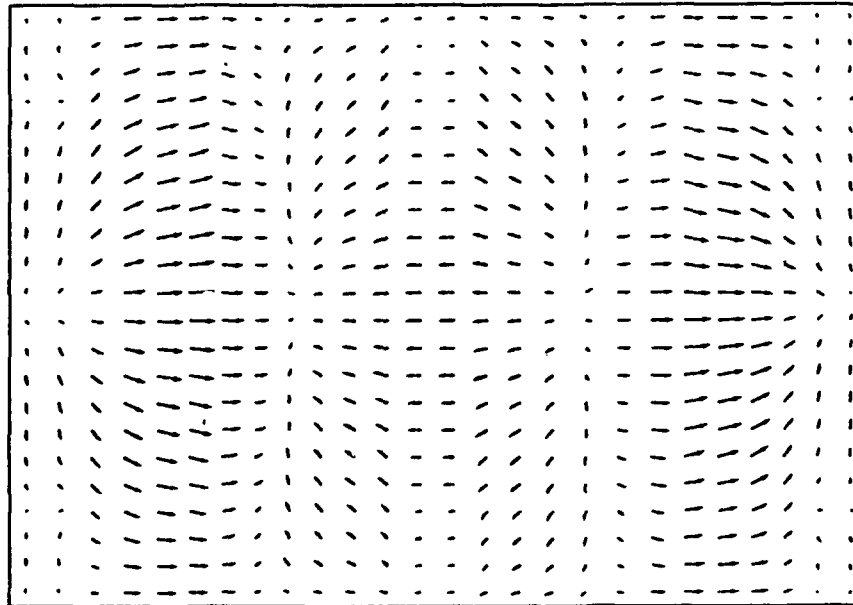


Figure 5b. In-phase and Quadrature Phase Current Components for the 15:th Natural Mode.
Corresponding to the TM₅₀₀ Cavity Mode.

Figures 6 through 7 compare the SEM and MoM radar cross section ($\sigma_{\theta\theta}$) predictions for the air loaded patch of Figure 1 using seven poles and natural modes. The RCS was calculated at 101 frequencies in all cases to produce a fairly smooth curve. Note that as more matching points are added the quality of the radar cross section prediction improves. This implies that a slight decrease in approximation accuracy at one or two frequencies is traded for a greatly improved average accuracy over a wider band.

Table 1. Cavity Resonances and Corresponding Complex Poles

Pole number	Mode indices (p, q, 0)	Cavity resonance (GHz)	Complex Pole (GHz)
1	100	3.93	3.811+j0.515
2	010	5.54	5.207+j0.1463
3	110	6.79	6.532+j0.0997
4	200	7.87	7.631+j0.1658
5	210	9.62	9.343+j0.1488
6	020	11.1	10.506+j0.3794
7	120	11.75	11.200+j0.3324
-	300	11.80	?
8	310	13.0	12.636+j0.2323
9	220	13.6	13.087+j0.3125
10	400	15.7	15.079+j0.3551
11	320	16.2	15.634+j0.3403
12	410	16.7	16.049+j0.3141
13	030	16.6	16.219+j0.5028
-	130	17.1	?
14	230	18.4	17.566+j0.4847
-	420	19.2	?
15	500	19.7	18.561+j0.3965

A detailed picture of the quality of the current approximation obtainable with seven modes is given in Figure 8 which compares the patch current J_{SEM} at 10 GHz with the 'true' patch current J_{MOM} as computed by the MoM. The relative error was

$$\epsilon_{rel} = \frac{|J_{SEM} - J_{MOM}|^2}{|J_{SEM}|^2} \approx 0.24.$$

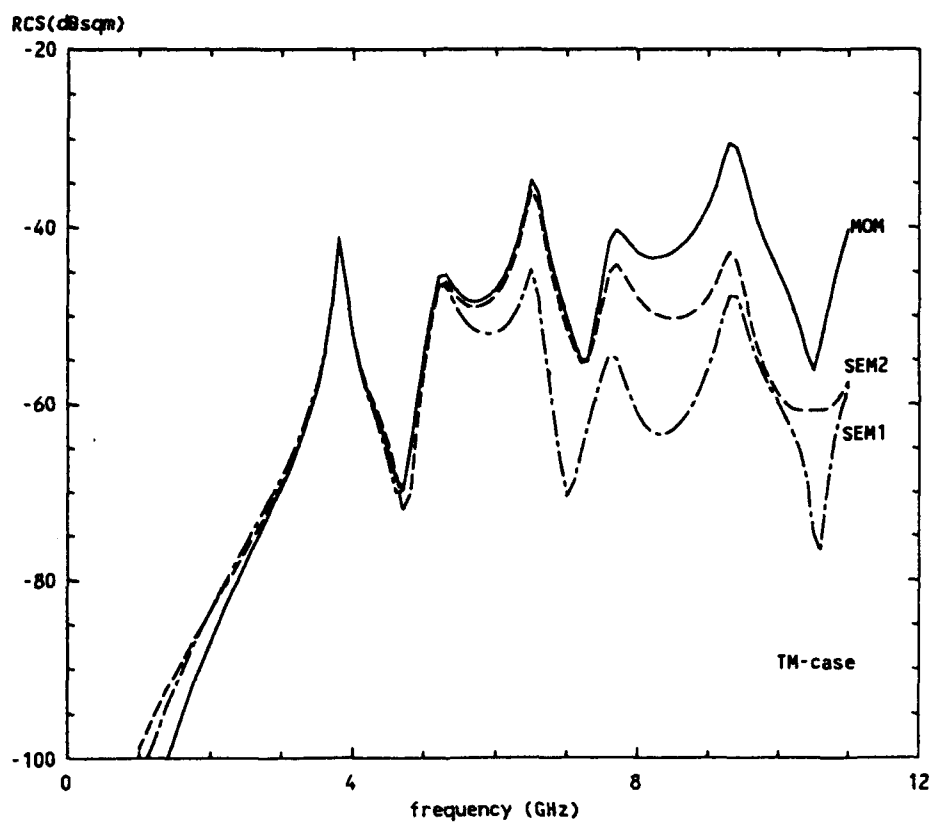


Figure 6. Comparison of the RCS Calculated Using the SEM Current Model and the Exact MoM Model for the Patch of Figure 1. The SEM current model is matched to the MoM currents at one frequency (4 GHz / curve SEM1) and two frequencies (4, 6 GHz / curve SEM2). Incident and scattered fields TM to the z-axis.

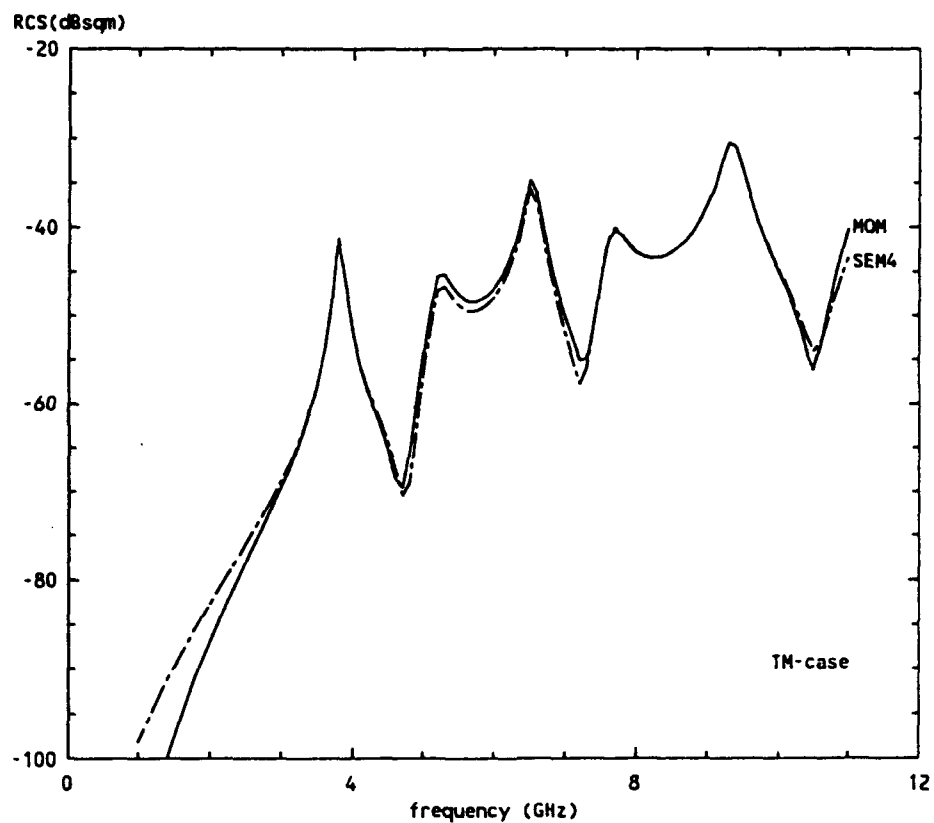
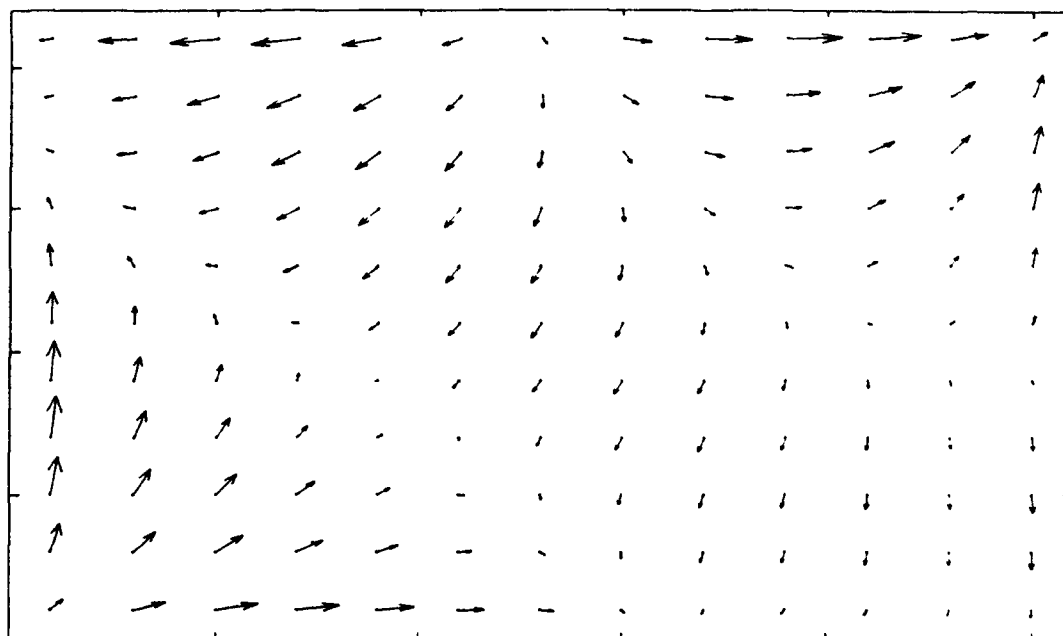
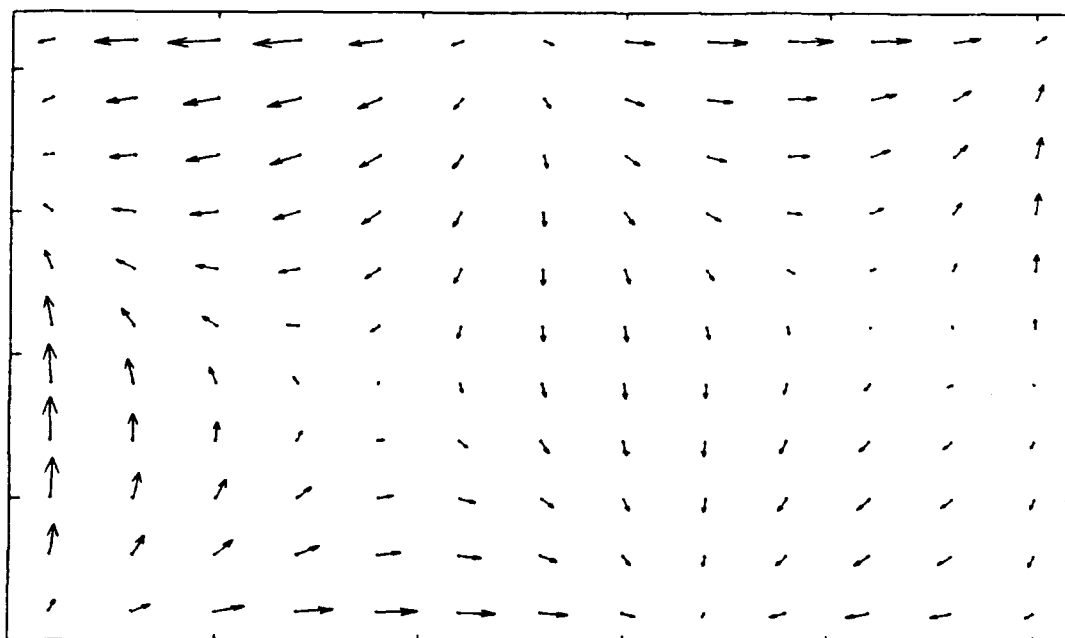


Figure 7. Comparison of the RCS Calculated Using the SEM Current Model and the Exact MoM Model for the Patch of Figure 1. The SEM current model is matched to the MoM currents at four frequencies (4, 6, 8, 10 GHz / curve SEM4). Incident and scattered fields TM to the z-axis.



MoM



SEM

Figure 8. In-phase Components of Patch Current as Obtained With Exact MoM Computation (Top) and With a Seven Mode Expansion (Bottom), at 10 GHz. Incident field TM to the z-axis.

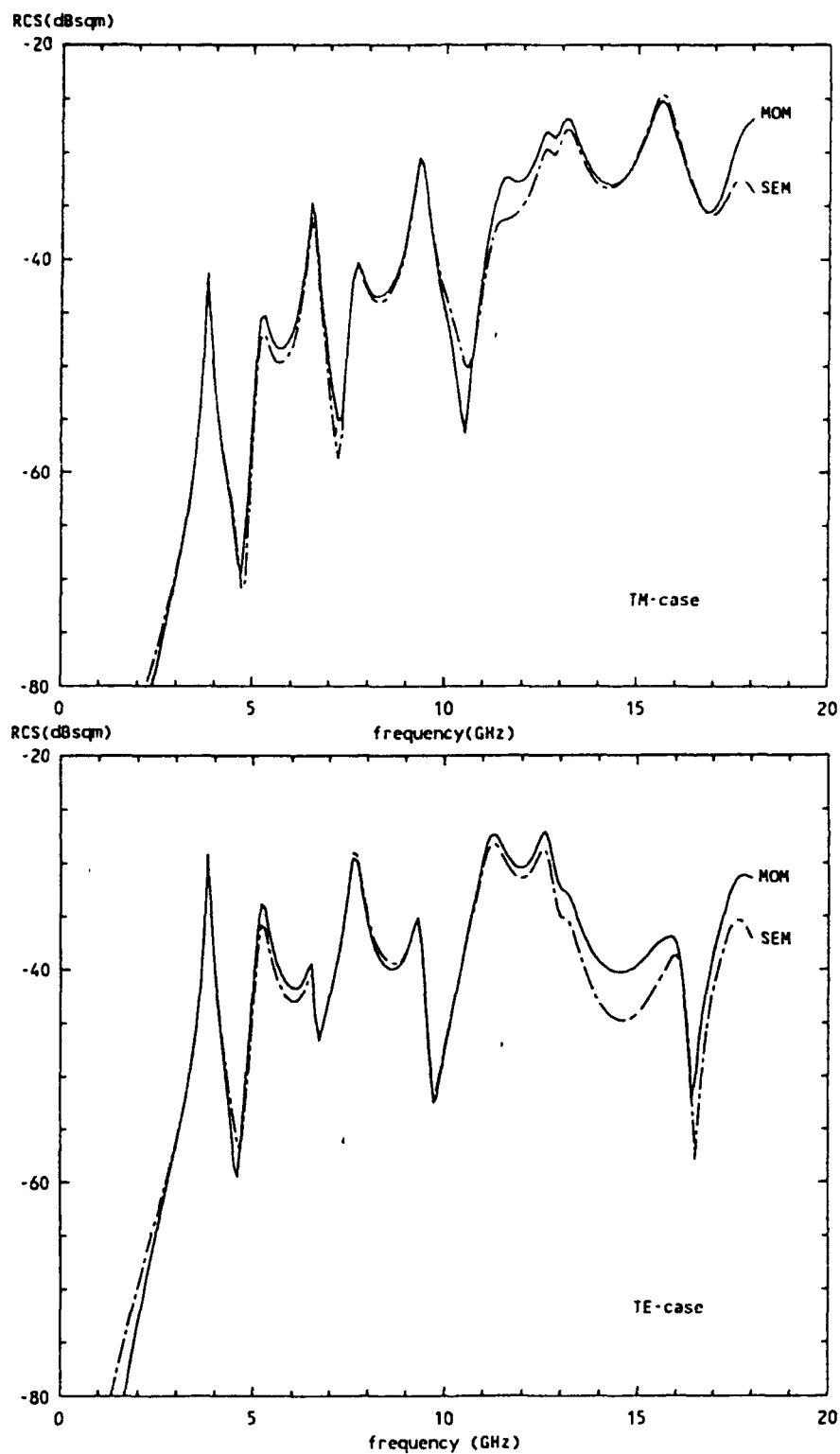


Figure 9. Comparison of the RCS Calculated Using the SEM Current Model and the Exact MoM Model for the Patch of Figure 1. The SEM current model includes 15 natural modes and is matched to the MoM currents at eight frequencies (2, 4, 6, 8, 10, 12, 14, 16 GHz). Incident and scattered fields TM (top) and TE (bottom) with respect to the z-axis.

Although in this case we matched at one frequency only, this is also a typical value when matching at several frequencies.

It is noteworthy that the high frequency limit of the current spectrum can be readily extended with more poles and natural modes. The use of 15 poles and modes in the current expansion \mathbf{J}_{SEM} gives excellent agreement between the corresponding radar cross section and the MoM computation up to about 18 GHz as shown in Figure 9. The small difference observed in Figure 9 (top) between 11-12 GHz may be an effect of the missing counterpart of the (300)-cavity resonance, which we were unable to find in the complex plane. Likewise the increasing difference between the two curves at the high frequency end is due to an incomplete number of poles in that vicinity. (In this example the MoM values may have somewhat reduced accuracy since at 18 GHz only 6 basis functions per wavelength are used. However, this is less important since the present purpose is to show only that the natural mode expansion does approximate the MoM curve well).

In the low frequency regime below the first resonance, the radar cross section of the patch varies theoretically as k^8 (24 dB per octave), as shown in Appendix A. The MoM based curve follows this behavior. The natural mode expansion as described by Eq. (1) however, does not, naturally have the correct low frequency behavior, in fact it does not even go to zero when the frequency is zero. By expanding the array factor of Eq. (9) in a Taylor series about $k_0 = 0$ it can be shown that the correct k_0 -dependence requires

$$\begin{aligned}\mathbf{J}_{\text{SEM}}(\mathbf{r}', \omega = 0) &= 0 \\ \frac{\partial \mathbf{J}_{\text{SEM}}(\mathbf{r}', \omega = 0)}{\partial \omega} &= 0\end{aligned}\tag{10}$$

but, unfortunately, these additional conditions are not readily imposed on \mathbf{J}_{SEM} . A partial correction is obtained by subtracting the DC-value $\mathbf{J}_{\text{SEM}}(\mathbf{r}', \omega=0)$ from the natural mode expansion (1). This leads to a k_0^6 -dependence but does not seem to significantly improve the overall approximation accuracy, as shown in Figure 10.

Finally, we note that once the patch current is available the radiation pattern or bistatic radar cross section for any desired direction is easily computed. An example of the bistatic RCS of the patch at 16 GHz is given in Figure 11. This frequency is sufficiently high for the scattering pattern to exhibit several lobes and these are apparently quite well reproduced by the natural mode expansion.

5. CONCLUSION

A method that uses existing frequency domain MoM codes to obtain a wideband characterization of three-dimensional antennas or scatterers has been developed. The codes must be extended to complex frequencies, although, in general, this is a simple matter. The resulting

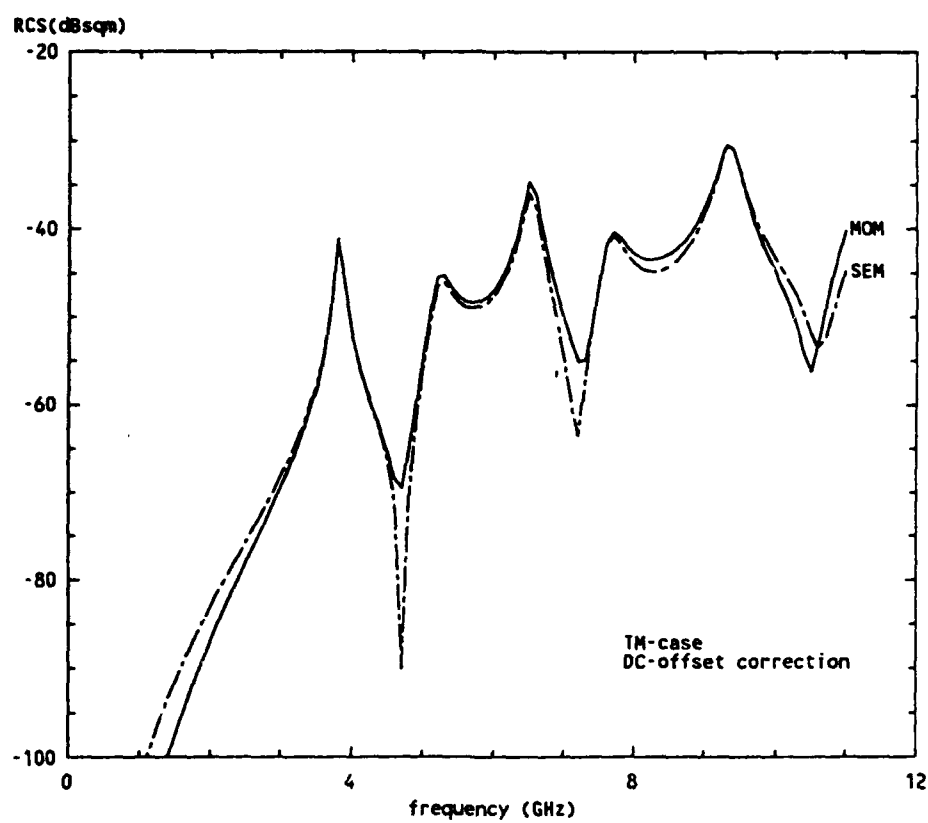


Figure 10. Same Case as Figure 7, Except That the SEM Current Model Has Been Modified to Include a DC Correction Term.

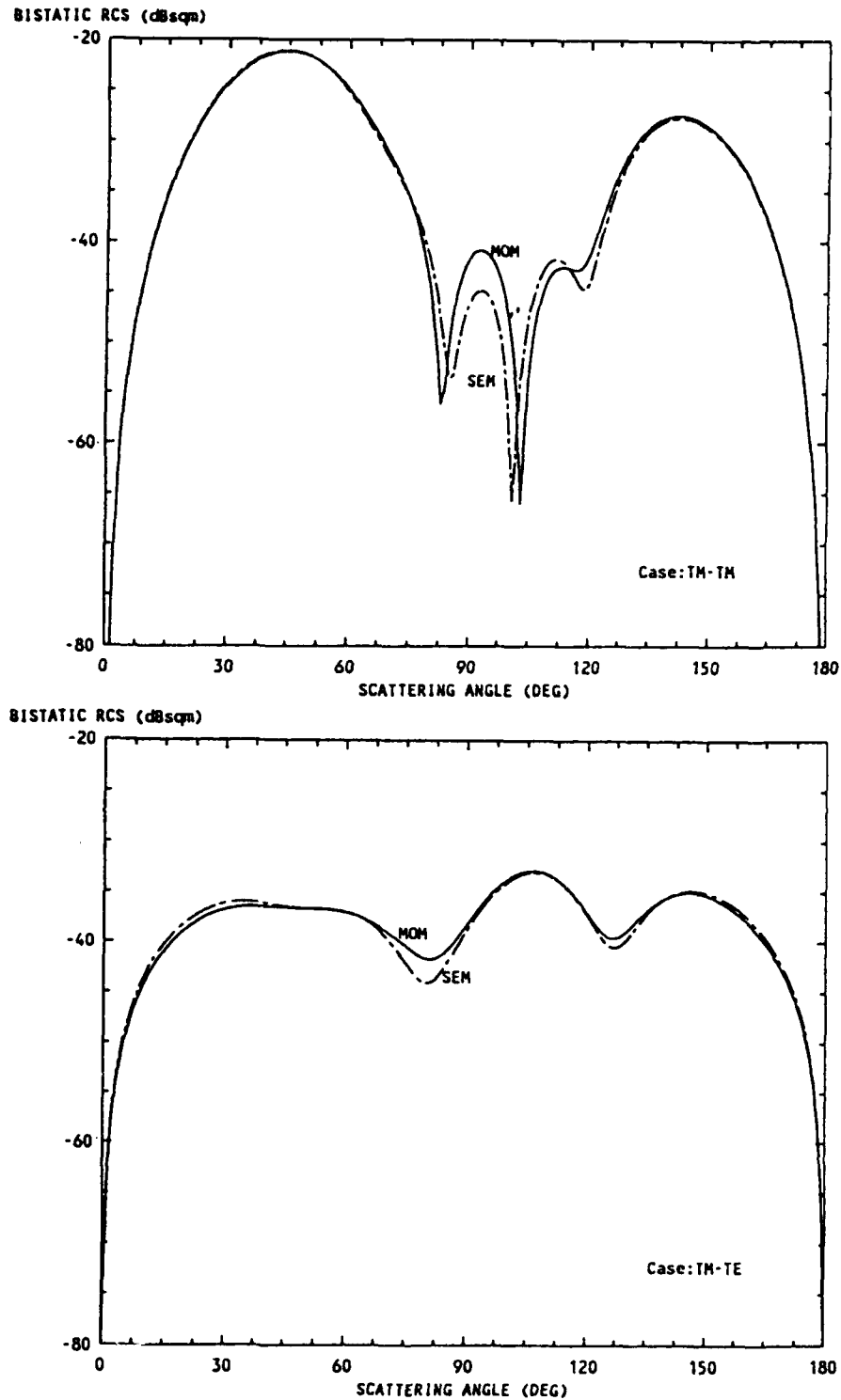


Figure 11. Bistatic RCS at 16 GHz Calculated Using the SEM Current Model and the Exact MoM Model for the Patch in Figure 1. The scattering angle is measured in the plane of incidence, with 30° being the direction of specular reflection. TM-TM and TM-TE denote co- and cross-polarized RCS, resp.

current model is very concise and numerically efficient. For example, we used only 7 current vectors to represent the complex spectrum shown in Figure 7, as compared to the 100 vectors required by conventional dense sampling.

The natural frequencies and modes provide a complete analytical model from which the complex time domain responses are readily obtained over all angles. A change in incidence angle requires a recomputation of the mode amplitudes only, which is a minimal computational effort.

In the example considered we obtained an accurate analytic representation for the spectrum of the patch current up to 18 GHz, which is commensurate with a spatial pulse width $\Delta x = c \Delta t \approx c / f_{\max} \approx 1.7$ cm, or about half the scatterer length (3.66 cm). Thus we are beginning to actually resolve the scatterer spatially and are doing considerably better than a 'late time' response, valid only after the pulse has painted over the entire object.

The method has been shown to work well for three dimensional structures, which are highly resonant, i.e., with poles close to the real axis. It remains to be seen what the effects of a lower Q would be.

At this point it is premature to compare the computer times of the proposed approach, based on a natural mode expansion, with a straightforward MoM approach, using dense frequency sampling. In our approach most of the computer time was expended in searching the complex plane for the natural resonances for which we used standard routines from a computer library. In contrast, the MoM codes have been highly optimized for computational efficiency. Thus the key to the overall success of the proposed method is an efficient root finding routine and there is both the need and the room for significant improvement in this respect.

References

1. Baum, C.E. (1976) The singularity expansion method, in *Transient Electromagnetic Fields* (L.B. Felsen, ed.) Chapter 3, Berlin: Springer Verlag.
2. Miller, E.K. (1991) Model-based parameter-estimation applications in electromagnetics, in *Electromagnetic Modeling and Measurements for Analysis and Synthesis Problems* (B. de Neumann, ed.). The Netherlands: Kluwer Academic Publishers.
3. Hanson, G.W., and Nyquist, D.P. (1993) The RCS of a Microstrip Dipole Deduced from an Expansion of Pole Singularities, *IEEE Trans. Antennas Propagat.*, **AP-41**, (no.3): 376-379.
4. Newman, E.H., and Forrai, D. (1987) Scattering from a microstrip patch, *IEEE Trans. Antennas and Propagat.*, **AP-35**, (no. 3): 245-251.
5. Aberle, J.T., Pozar, D.M., and Birtcher, C.R. (1991) Evaluation of input impedance and radar cross section of probe-fed microstrip patch elements using an accurate feed model, *IEEE Trans. Antennas and Propagat.*, **AP-39**, (no.12): 1991-1996.
6. Mosig, J.R., and Gardiol, F.E. (1982) A dynamical radiation model for microstrip structures, in *Advances in Electronics and Electron Physics*, vol. 59, pp. 139-237, New York: Academic Press.
7. Mosig, J.R., Hall, R.C., and Gardiol, F.E. (1989) Numerical analysis of microstrip patch antennas, in *The Handbook of Microstrip Antennas* (J.R. James and P.S. Hall, eds.), Chapter 8, U.K.: Peter Peregrinus Press.
8. Press, W.H., Flannery, B.P., Teukolsky, S.A., and Vetterling, W.T. (1986) *Numerical Recipes, The Art of Scientific Computing*. Cambridge, England: Cambridge University Press.
9. Donagarrá, J.J., et al., (1979) *LINPACK User's Guide*. Philadelphia: Society for Industrial and Applied Mathematics.
10. Van Bladel, J. (1985) *Electromagnetic Fields*. Springer-Verlag, Berlin, p 215.

Appendix

The k_0 -dependence of the Radar Cross Section of a Microstrip Patch at Low Frequencies

The scattering from a metallic plate over a reflecting ground plane can be analyzed in terms of scattering from two plates in free space that are illuminated from above and below. In the upper half-space the total fields are identical for the original and equivalent problems shown in Figure A1.

First consider a single plane wave incident on the equivalent structure from above. For low frequencies the current on the upper patch can be expanded as

$$\mathbf{J}' = \mathbf{J}'_0 + k_0 \mathbf{J}'_1 + k_0^2 \mathbf{J}'_2 + \dots \quad (\text{A1a})$$

and on the lower patch

$$\mathbf{J}'' = \mathbf{J}''_0 + k_0 \mathbf{J}''_1 + k_0^2 \mathbf{J}''_2 + \dots \quad (\text{A1b})$$

where k_0 is the wavenumber. The first terms in each expansion are the same since both patches have the same currents as $k_0 \rightarrow 0$.

For incidence from below, due to symmetry and the sign reversal of the incident field, the upper patch will carry the current $-\mathbf{J}''$ and the lower $-\mathbf{J}'$. Superimposing these two cases leads to upper and lower patch currents $\Delta\mathbf{J}$ and $-\Delta\mathbf{J}$, respectively, where

$$\Delta\mathbf{J} = k_0 (\mathbf{J}'_1 - \mathbf{J}''_1). \quad (\text{A2})$$

The vector potential due to currents on the equivalent structure is

$$\mathbf{A} = \frac{\mu_0}{4\pi} \int_{S_1 + S_2} \mathbf{J} \frac{e^{-jk_0 r}}{r} dS \quad (\text{A3})$$

where the integration is over both patches S_1 and S_2 . Substituting the patch currents above,

using the fact that the patch dimensions are small relative to the wavelength, and making the usual far field approximations leads to

$$\mathbf{A} \approx \frac{\mu_0}{4\pi} \frac{e^{-jk_0 r}}{r} (-j2k_0 h \cos\theta) \int_{S_1} \Delta \mathbf{J} dS. \quad (\text{A4})$$

We must now determine the k_0 -dependence of the integral appearing in Eq. (A4).

For a single incident plane wave the patch currents are equal to first order and thus the far-field vector potential at low frequencies becomes

$$\mathbf{A} \approx \frac{\mu_0}{4\pi} \frac{e^{-jk_0 r}}{r} \int_{S_1} \mathbf{J}_0 dS \quad (\text{A5})$$

The electric far field is proportional to k_0 times the vector potential

$$\begin{aligned} E_\phi &\propto k_0 A_\phi \\ E_\theta &\propto k_0 A_\theta \end{aligned} \quad (\text{A6})$$

and from Rayleigh scattering theory we know

$$\begin{aligned} E_\theta &\propto k_0^2 \\ E_\phi &\propto k_0^2 \end{aligned} \quad (\text{A7})$$

This leads to the result that the integral appearing in Eq. (A5) is proportional to k_0 :

$$\int_{S_1} \mathbf{J}_0 dS \propto k_0 \quad (\text{A8})$$

Since the integrals over \mathbf{J}_0 and \mathbf{J}_1' , \mathbf{J}_1'' are of the same order as k_0 , the integral in Eq. (A4) is proportional to k_0^2 .

$$\int_{S_1} \Delta \mathbf{J} dS = k_0 \int_{S_1} (\mathbf{J}_1' - \mathbf{J}_1'') dS \propto k_0^2 \quad (\text{A9})$$

Substituting Eq. (A9) in Eq. (A4) and using Eq. (A6) leads to a far field for the patch over a ground plane

$$E_{\theta} \propto k_0^4$$

$$E_{\phi} \propto k_0^4 \quad (10)$$

and a low frequency radar cross section proportional to k_0^8

$$\sigma(\theta, \phi) \propto k_0^8. \quad (A11)$$

This corresponds to a roll-off of 24 dB per octave.

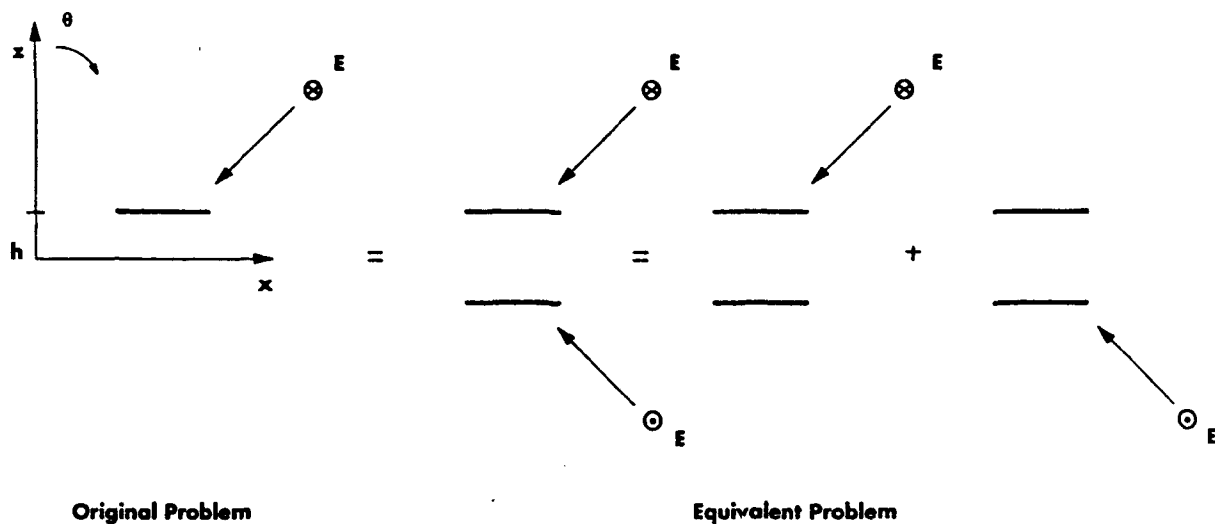


Figure A1. Scattering From a Microstrip Patch Related to a Patch Pair in Free Space.

**MISSION
OF
ROME LABORATORY**

Rome Laboratory plans and executes an interdisciplinary program in research, development, test, and technology transition in support of Air Force Command, Control, Communications and Intelligence (C3I) activities for all Air Force platforms. It also executes selected acquisition programs in several areas of expertise. Technical and engineering support within areas of competence is provided to ESC Program Offices (POs) and other ESC elements to perform effective acquisition of C3I systems. In addition, Rome Laboratory's technology supports other AFMC Product Divisions, the Air Force user community, and other DOD and non-DOD agencies. Rome Laboratory maintains technical competence and research programs in areas including, but not limited to, communications, command and control, battle management, intelligence information processing, computational sciences and software producibility, wide area surveillance/sensors, signal processing, solid state sciences, photonics, electromagnetic technology, superconductivity, and electronic reliability/maintainability and testability.